Eur. Phys. J. C 40, 555–564 (2005)
Digital Object Identifier (DOI) 10.1140/epjc/s2005-02145-9

THE EUROPEAN PHYSICAL JOURNAL C

H/A Higgs mixing in CP-noninvariant supersymmetric theories

S.Y. Choi[1], J. Kalinowski[2,a], Y. Liao[3], P.M. Zerwas[4]

[1] Department of Physics, Chonbuk National University, Chonju 561-756, Korea
[2] Institute of Theoretical Physics, Warsaw University, 00681 Warsaw, Poland
[3] Institut für Theoretische Physik, Universität Leipzig, 04109 Leipzig, Germany
[4] Deutsches Elektronen-Synchrotron DESY, 22603 Hamburg, Germany

Received: 1 October 2004 / Revised version: 10 January 2005 /
Published online: 9 March 2005 –

Abstract. For large masses, the two heavy neutral Higgs bosons are nearly degenerate in many 2-Higgs doublet models, and particularly in supersymmetric models. In such a scenario the mixing between the states can be very large if the theory is CP-noninvariant. We analyze the formalism describing this configuration, and we point to some interesting experimental consequences.

1 Introduction

At least two iso-doublet scalar fields must be introduced in supersymmetric theories to achieve a consistent formulation of the Higgs sector. Supersymmetric theories in minimal form are specific realizations of general scenarios which include two doublets in the Higgs sector. After three fields are absorbed to generate the masses of the electroweak gauge bosons, five fields are left that give rise to physical particles. In CP-invariant theories, besides the charged states, two of the three neutral states are CP-even, while the third is CP-odd. In CP-noninvariant theories the three neutral states however mix to form a triplet with even and odd components in the wave-functions under CP-transformations [1–5]. As expected from general quantum mechanical rules, the mixing can become very large if the states are nearly mass-degenerate. This situation is naturally realized for supersymmetric theories in the decoupling limit in which two of the neutral states are heavy.

In this note we analyze H/A mixing in a simple quantum mechanical formalism that reveals the underlying structure in a clear and transparent way. H and A represent two heavy nearly mass-degenerate fields. After the discussion of the general CP-noninvariant 2-Higgs doublet model (2HDM), we adopt the minimal supersymmetric standard model, though extended to a CP-noninvariant version [MSSM-CP], as a well-motivated example for the analysis.

2 Complex mass matrix

The most general form of the self-interaction of 2-Higgs doublets in a CP-noninvariant theory is described by the potential [6]

$$\begin{aligned}\mathcal{V} = {} & m_{11}^2 \Phi_1^\dagger \Phi_1 + m_{22}^2 \Phi_2^\dagger \Phi_2 - \left[m_{12}^2 \Phi_1^\dagger \Phi_2 + \text{h.c.} \right] \\ & + \frac{1}{2}\lambda_1 \left(\Phi_1^\dagger \Phi_1 \right)^2 + \frac{1}{2}\lambda_2 \left(\Phi_2^\dagger \Phi_2 \right)^2 \\ & + \lambda_3 \left(\Phi_1^\dagger \Phi_1 \right) \left(\Phi_2^\dagger \Phi_2 \right) + \lambda_4 \left(\Phi_1^\dagger \Phi_2 \right) \left(\Phi_2^\dagger \Phi_1 \right) \\ & + \Big\{ \frac{1}{2}\lambda_5 \left(\Phi_1^\dagger \Phi_2 \right)^2 \\ & \quad + \left[\lambda_6 \left(\Phi_1^\dagger \Phi_1 \right) + \lambda_7 \left(\Phi_2^\dagger \Phi_2 \right) \right] \Phi_1^\dagger \Phi_2 + \text{h.c.} \Big\}, \end{aligned} \quad (1)$$

where $\Phi_{1,2}$ denote two complex $Y = 1$, $\mathrm{SU}(2)_\mathrm{L}$ iso-doublet scalar fields. The coefficients are in general all non-zero. The parameters $m_{12}^2, \lambda_{5,6,7}$ can be complex, incorporating the CP-noninvariant elements in the interactions:

$$m_{12}^2 = m_{12}^{2\mathrm{R}} + \mathrm{i} m_{12}^{2\mathrm{I}}, \quad \lambda_{5,6,7} = \lambda_{5,6,7}^\mathrm{R} + \mathrm{i}\lambda_{5,6,7}^\mathrm{I}\,. \quad (2)$$

Assuming the scalar fields to develop non-zero vacuum expectation values to break the electroweak symmetries but leaving $\mathrm{U}(1)_\mathrm{EM}$ invariant, the vacuum fields can be defined as

$$\langle \Phi_1 \rangle = \frac{v_1}{\sqrt{2}} \begin{pmatrix} 0 \\ 1 \end{pmatrix}, \quad \langle \Phi_2 \rangle = \frac{v_2}{\sqrt{2}} \begin{pmatrix} 0 \\ 1 \end{pmatrix}. \quad (3)$$

Without loss of generality, the two vacuum expectation values v_i $[i = 1, 2]$ can be chosen real and positive after an appropriate global $\mathrm{U}(1)$ phase rotation; the parameters of the (effective) potential (1) are defined after this rotation. As usual,

$$v = \sqrt{v_1^2 + v_2^2} = 1/\sqrt{\sqrt{2} G_\mathrm{F}} \ \text{ and } \ \tan\beta = v_2/v_1, \quad (4)$$

[a] e-mail: jan.kalinowski@fuw.edu.pl

with $v \approx 246\,\mathrm{GeV}$. The abbreviations $t_\beta = \tan\beta$, $c_\beta = \cos\beta$, $s_{2\beta} = \sin 2\beta$ etc. will be used from now on.

The conditions for minimizing the potential (1) relate the parameters m_{ii}^2 to the real part of m_{12}^2, λ_k, v and t_β:

$$\begin{aligned} m_{11}^2 &= m_{12}^{2\mathrm{R}} t_\beta \\ &\quad -\frac{1}{2}v^2\left[\lambda_1 c_\beta^2 + \lambda_{345} s_\beta^2 + 3\lambda_6^{\mathrm{R}} s_\beta c_\beta + \lambda_7^{\mathrm{R}} s_\beta^2 t_\beta\right], \\ m_{22}^2 &= m_{12}^{2\mathrm{R}} t_\beta^{-1} \\ &\quad -\frac{1}{2}v^2\left[\lambda_1 s_\beta^2 + \lambda_{345} c_\beta^2 + \lambda_6^{\mathrm{R}} c_\beta^2 t_\beta^{-1} + 3\lambda_7^{\mathrm{R}} s_\beta c_\beta\right], \end{aligned} \tag{5}$$

with the abbreviation $\lambda_{345} = \lambda_3 + \lambda_4 + \lambda_5^{\mathrm{R}}$, and the imaginary part of m_{12}^2 to the imaginary parts of the $\lambda_{5,6,7}$ parameters:

$$m_{12}^{2\mathrm{I}} = \frac{1}{2}v^2\left[\lambda_5^{\mathrm{I}} s_\beta c_\beta + \lambda_6^{\mathrm{I}} c_\beta^2 + \lambda_7^{\mathrm{I}} s_\beta^2\right]. \tag{6}$$

It will prove convenient later to exchange the real part of m_{12}^2 for the auxiliary parameter M_A^2, or in units of v, $m_A^2 = M_A^2/v^2$, defined by the relation

$$m_{12}^{2\mathrm{R}} = \frac{1}{2}v^2\left[m_A^2 s_{2\beta} + \lambda_5^{\mathrm{R}} s_{2\beta} + \lambda_6^{\mathrm{R}} c_\beta^2 + \lambda_7^{\mathrm{R}} s_\beta^2\right]. \tag{7}$$

This parameter will turn out to be one of the key parameters in the system.

In a first step the $\Phi_{1,2}$ system is rotated to the Higgs basis $\Phi_{a,b}$,

$$\begin{aligned} \Phi_a &= \quad \cos\beta\,\Phi_1 + \sin\beta\,\Phi_2, \\ \Phi_b &= -\sin\beta\,\Phi_1 + \cos\beta\,\Phi_2, \end{aligned} \tag{8}$$

which is built up by the two iso-spinors:

$$\begin{aligned} \Phi_a &= \begin{pmatrix} G^+ \\ \frac{1}{\sqrt{2}}\left(v + H_a + \mathrm{i}G^0\right) \end{pmatrix}, \\ \Phi_b &= \begin{pmatrix} H^+ \\ \frac{1}{\sqrt{2}}\left(H_b + \mathrm{i}A\right) \end{pmatrix}. \end{aligned} \tag{9}$$

The three fields $G^{\pm,0}$ can be identified as the would-be Goldstone bosons, while $H^\pm$, $H_{a,b}$ and A give rise to physical Higgs bosons. The charged Higgs mass $M_{H^\pm}$ and the real mass matrix $\mathcal{M}_{0\mathrm{R}}^2$ of neutral Higgs fields in the basis of H_a, H_b, A can easily be derived from the potential after the rotations:

$$M_{H^\pm}^2 = M_A^2 + \frac{1}{2}\,v^2\lambda_F \tag{10}$$

and

$$\mathcal{M}_{0\mathrm{R}}^2 = v^2\begin{pmatrix} \lambda & -\hat\lambda & -\hat\lambda_p \\ & \lambda - \lambda_A + m_A^2 & -\lambda_p \\ & & m_A^2 \end{pmatrix}, \tag{11}$$

abbreviated for easier reading and to be complemented symmetrically. The notation for the real parts of the couplings,

$$\begin{aligned} \lambda &= \lambda_1 c_\beta^4 + \lambda_2 s_\beta^4 + \frac{1}{2}\lambda_{345} s_{2\beta}^2 + 2 s_{2\beta}\left(\lambda_6^{\mathrm{R}} c_\beta^2 + \lambda_7^{\mathrm{R}} s_\beta^2\right), \\ \hat\lambda &= \frac{1}{2}s_{2\beta}\left[\lambda_1 c_\beta^2 - \lambda_2 s_\beta^2 - \lambda_{345} c_{2\beta}\right] \\ &\quad -\lambda_6^{\mathrm{R}} c_\beta c_{3\beta} - \lambda_7^{\mathrm{R}} s_\beta s_{3\beta}, \\ \lambda_A &= c_{2\beta}\left(\lambda_1 c_\beta^2 - \lambda_2 s_\beta^2\right) + \lambda_{345} s_{2\beta}^2 - \lambda_5^{\mathrm{R}} \\ &\quad +2\lambda_6^{\mathrm{R}} c_\beta s_{3\beta} - 2\lambda_7^{\mathrm{R}} s_\beta c_{3\beta}, \\ \lambda_F &= \lambda_5^{\mathrm{R}} - \lambda_4, \end{aligned} \tag{12}$$

essentially follows [6], and

$$\begin{aligned} \lambda_p &= \frac{1}{2}\lambda_5^{\mathrm{I}} c_{2\beta} - \frac{1}{2}\left(\lambda_6^{\mathrm{I}} - \lambda_7^{\mathrm{I}}\right) s_{2\beta}, \\ \hat\lambda_p &= \frac{1}{2}\lambda_5^{\mathrm{I}} s_{2\beta} + \lambda_6^{\mathrm{I}} c_\beta^2 + \lambda_7^{\mathrm{I}} s_\beta^2 \quad \left[= 2m_{12}^{2\mathrm{I}}/v^2\right] \end{aligned} \tag{13}$$

are introduced for the imaginary parts of the couplings [7].

In a CP-invariant theory all couplings are real and the off-diagonal elements $\lambda_p, \hat\lambda_p$ vanish. In this case the neutral mass matrix separates into the standard CP-even 2×2 part and the standard [stand-alone] CP-odd part.[1] The parameter M_A is then identified as the mass of the CP-odd Higgs boson A. The 2×2 submatrix of the H_a and H_b system can be diagonalized, leading to the two CP-even neutral mass eigenstates $h,\ H$; in terms of H_a, H_b:

$$\begin{aligned} H &= \cos\gamma\, H_a - \sin\gamma\, H_b, \\ h &= \sin\gamma\, H_a + \cos\gamma\, H_b, \end{aligned} \tag{14}$$

with $\gamma = \beta - \alpha$; the angle α is the conventional CP-even neutral Higgs boson mixing angle in the $[\Phi_1, \Phi_2]$ basis of the CP-invariant 2HDM. The diagonalization of the mass matrix leads to the relation

$$\tan 2\gamma = \frac{2\hat\lambda}{\lambda_A - m_A^2}, \tag{15}$$

with $\gamma \in [0, \pi]$.

However, also in the general CP-noninvariant case, the fields $h_a = h, H, A$ serve as a useful basis, giving rise to the general final form of the real part of the neutral mass matrix $\mathcal{M}_{\mathrm{R}}^2$,

$$\begin{aligned} \mathcal{M}_{\mathrm{R}}^2 &= v^2 \\ &\times \begin{pmatrix} \lambda + (m_A^2 - \lambda_A)\, c_\gamma^2 c_{2\gamma}^{-1} & 0 & -\lambda_p\, c_\gamma - \hat\lambda_p\, s_\gamma \\ & \lambda - (m_A^2 - \lambda_A)\, s_\gamma^2 c_{2\gamma}^{-1} & \lambda_p\, s_\gamma - \hat\lambda_p\, c_\gamma \\ & & m_A^2 \end{pmatrix}, \end{aligned} \tag{16}$$

which is hermitian and symmetric by CPT invariance.

[1] The Goldstone bosons $G^{\pm,0}$ (carrying zero mass) decouple from the physical states.

This hermitian part (16) of the mass matrix is supplemented by the anti-hermitian part $-\mathrm{i}M\Gamma$ incorporating the decay matrix. This matrix includes the widths of the states $h_a = h, H, A$ in the diagonal elements as well as the transition elements within any combination of pairs. All these elements $(M\Gamma)^{AB}_{ab}$ are built up by loops of the fields (AB) in the self-energy matrix $\langle h_a h_b \rangle$ of the Higgs fields.

In general, the light Higgs boson, the fermions and electroweak gauge bosons, and in supersymmetric theories, gauginos, higgsinos and scalar states may contribute to the loops in the propagator matrix. In the decoupling limit explored later, the couplings of the heavy Higgs bosons to gauge bosons and their supersymmetric partners are suppressed. Assuming all supersymmetric particles to be suppressed either by couplings or by phase space in $M\Gamma$, we will consider only loops built up by the light Higgs boson and the top quark as characteristic examples; loops from other (s)particles could be treated in the same way of course.

(i) Light scalar Higgs h states

While the Hhh coupling is CP-conserving, the Ahh coupling is CP-violating. Expressed in terms of the λ parameters in the potential they are given as

$$\begin{aligned} g_{Hhh}/v = &-3\left(c_\beta c_\alpha s_\alpha^2 \lambda_1 + s_\beta s_\alpha c_\alpha^2 \lambda_2\right) \\ &-\lambda_{345}\left[c_\beta c_\alpha (3c_\alpha^2 - 2) + s_\beta s_\alpha (3s_\alpha^2 - 2)\right] \\ &-3\lambda_6^{\mathrm{R}}\left[s_\beta c_\alpha s_\alpha^2 + c_\beta s_\alpha (3s_\alpha^2 - 2)\right] \\ &-3\lambda_7^{\mathrm{R}}\left[c_\beta s_\alpha c_\alpha^2 + s_\beta c_\alpha \left(3c_\alpha^2 - 2\right)\right], \\ g_{Ahh}/v = &\ \lambda_5^{\mathrm{I}}\left(s_\beta c_\beta - 2 s_\alpha c_\alpha\right) \\ &+\lambda_6^{\mathrm{I}}\left[\left(1 + 2c_\beta^2\right) s_\alpha^2 - s_{2\beta} s_\alpha c_\alpha\right] \\ &+\lambda_7^{\mathrm{I}}\left[\left(1 + 2s_\beta^2\right) c_\alpha^2 - s_{2\beta} s_\alpha c_\alpha\right]. \end{aligned} \tag{17}$$

The trigonometric functions s_α and c_α can be re-expressed by the sine and cosine of β and γ after inserting $\alpha = \beta - \gamma$.

The imaginary part of the light Higgs loop is given for CP-conserving and CP-violating transitions by

$$\begin{aligned} (M\Gamma)^{hh}_{HH/AA} &= \frac{\beta_h}{32\pi} g^2_{Hhh/Ahh}, \\ (M\Gamma)^{hh}_{HA/AH} &= \frac{\beta_h}{32\pi} g_{Hhh} g_{Ahh}, \end{aligned} \tag{18}$$

where β_h denotes the velocity of the light Higgs boson h in the decays $H/A \to hh$ [with the heavy Higgs bosons assumed to be mass-degenerate].

(ii) Top-quark states

The Htt and Att couplings are defined by the Lagrangian

$$\mathcal{L}_t = H\bar{t}\left[s_H + \mathrm{i}\gamma_5 p_H\right] t + A\bar{t}\left[s_A + \mathrm{i}\gamma_5 p_A\right] t, \tag{19}$$

which includes the CP-conserving couplings[2] s_H, p_A and the CP-violating couplings p_H, s_A. For the top quark loop we find

$$\begin{aligned} (M\Gamma)^{tt}_{HH/AA} &= \frac{3M^2_{H/A}}{8\pi}\,\beta_t\, g^{tt}_{HH/AA}, \\ (M\Gamma)^{tt}_{HA/AH} &= \frac{3M^2_{H/A}}{8\pi}\,\beta_t\, g^{tt}_{HA/AH}, \end{aligned} \tag{20}$$

in the same notation as before. The transitions include incoherent and coherent mixtures of scalar and pseudoscalar couplings,

$$\begin{aligned} g^{tt}_{HH} &= \beta_t^2 s_H^2 + p_H^2, \\ g^{tt}_{AA} &= \beta_t^2 s_A^2 + p_A^2, \\ g^{tt}_{HA} &= g^{tt}_{AH} = \beta_t^2 s_H s_A + p_H p_A, \end{aligned} \tag{21}$$

where β_t denotes the velocity of the top quarks in the Higgs rest frame.

These loops also contribute to the real part of the mass matrix. They either renormalize the λ parameters of the Higgs potential or they generate such parameters if not present yet at the tree level. In the first case they do not modify the generic form of the mass matrix, and the set of renormalized λ's are interpreted as free parameters to be determined experimentally. The same procedure also applies to supersymmetric theories in which some of the λ's are generated radiatively by stop loops, introducing CP-violation into the Higgs sector through bilinear and trilinear interactions in the superpotential, a case discussed later in detail.

Including these elements, the final complex mass matrix can be written in the Weisskopf–Wigner form [8]

$$\mathcal{M}^2 = \mathcal{M}^2_{\mathrm{R}} - \mathrm{i}M\ \Gamma. \tag{22}$$

which will be diagonalized in the next section.

Decoupling limit

The decoupling limit [6] is defined by the inequality

$$M_A^2 \ \gg\ |\lambda_i|\, v^2 \tag{23}$$

with $|\lambda_i| \lesssim O(1)$ or $O(g^2, g'^2)$, g^2 and g'^2 denoting the electroweak gauge couplings. The limit is realized in many supersymmetric models, particularly in SUGRA models with $M_A^2 \gg v^2$. It is well known that in the decoupling limit the heavy states H and A, as well as $H^\pm$, are nearly mass-degenerate. This feature is crucial for large mixing effects between the CP-odd and CP-even Higgs bosons, A and H, analyzed in this report.

As the trigonometric sin/cos functions of $\gamma = \beta - \alpha$ approach the following values in the decoupling limit:

$$c_\gamma \simeq \hat{\lambda}/m_A^2 \to 0, \qquad s_\gamma \to 1 \tag{24}$$

up to second order in $1/m_A^2$, the real part of the complex mass matrix acquires the simple form

$$\mathcal{M}^2_{\mathrm{R}} \simeq v^2 \begin{pmatrix} \lambda & 0 & -\hat{\lambda}_p \\ 0 & m_A^2 + \lambda - \lambda_A & \lambda_p \\ -\hat{\lambda}_p & \lambda_p & m_A^2 \end{pmatrix} \tag{25}$$

[2] In the type-II class of CP-conserving 2-Higgs doublet models, to which the minimal supersymmetric extension of the standard model belongs, the two couplings s_H, p_A approach equal values, $\simeq \cot\beta\, m_t/v$, for large Higgs masses.

in the leading order $\sim m_A^2$ and next-to-leading order ~ 1. The Hhh and Ahh couplings are simplified in the decoupling limit and they can be written in the condensed form:

$$\begin{aligned} g_{Hhh}/v \to & -\frac{3}{2}s_{2\beta}\left(c_\beta^2\lambda_1 - s_\beta^2\lambda_2 - c_{2\beta}\lambda_{345}\right) \\ & +3\left(c_\beta c_{3\beta}\lambda_6^{\rm R} + s_\beta s_{3\beta}\lambda_7^{\rm R}\right) \\ \to & -3\lambda_7^{\rm R}, \\ g_{Ahh}/v \to & \frac{3}{2}s_{2\beta}\lambda_5^{\rm I} + 3\left(c_\beta^2\lambda_6^{\rm I} + s_\beta^2\lambda_7^{\rm I}\right) \\ \to & +3\lambda_7^{\rm I}, \end{aligned} \tag{26}$$

since in this limit we can set $c_\alpha = s_\beta$ and $s_\alpha = -c_\beta$. The couplings simplify further for moderately large $\tan\beta$ and they are determined in this range by the coefficient λ_7 alone as demonstrated above.

3 Physical masses and states

Following the steps in the appendix of [9], it is easy to prove mathematically, that mixing between the light Higgs state and the heavy Higgs states is small, but large between the two nearly mass-degenerate states. Mathematically the mixing effects are of the order of the off-diagonal elements in the mass matrix normalized to the difference of the (complex) mass-squared eigenvalues. On quite general grounds, this is a straightforward consequence of the uncertainty principle. We can therefore restrict ourselves to the discussion of the mass-degenerate 2×2 system of the heavy Higgs bosons H, A, allowing us to reduce the calculational effort to a minimum.

If the mass differences become small, the mixing of the states is strongly affected by the widths of the states and the complex Weisskopf–Wigner mass matrix $\mathcal{M}^2 = \mathcal{M}^2_{\rm R} - {\rm i}M\Gamma$ must be considered in total, not only the real part. This is well known in the literature from resonance mixing [10] and has recently also been recognized for the Higgs sector [11].

By CPT invariance, the complex mass matrix $\mathcal{M}^2$ is symmetric. Adopting the notation in [10] for the H/A submatrix which is separated in the lower right corner of (25),

$$\mathcal{M}^2_{HA} = \begin{pmatrix} M_H^2 - {\rm i}M_H\Gamma_H & \Delta^2_{HA} \\ \Delta^2_{HA} & M_A^2 - {\rm i}M_A\Gamma_A \end{pmatrix}, \tag{27}$$

the matrix can be diagonalized,

$$\mathcal{M}^2_{H_iH_j} = \begin{pmatrix} M_{H_2}^2 - {\rm i}M_{H_2}\Gamma_{H_2} & 0 \\ 0 & M_{H_3}^2 - {\rm i}M_{H_3}\Gamma_{H_3} \end{pmatrix} \tag{28}$$

through a *rotation by a complex mixing angle*:

$$\mathcal{M}^2_{H_iH_j} = C\mathcal{M}^2_{HA}C^{-1}, \quad C = \begin{pmatrix} \cos\theta & \sin\theta \\ -\sin\theta & \cos\theta \end{pmatrix}, \tag{29}$$

with

$$X = \frac{1}{2}\tan 2\theta = \frac{\Delta^2_{HA}}{M_H^2 - M_A^2 - {\rm i}\left[M_H\Gamma_H - M_A\Gamma_A\right]}\,. \tag{30}$$

A non-vanishing (complex) mixing parameter $\Delta^2_{HA} \neq 0$ requires CP-violating transitions between H and A either in the real mass matrix, $\lambda_p \neq 0$, or in the decay mass matrix, $\Gamma_{HA} \neq 0$, [or both]. When, in the decoupling limit, the masses M_H and M_A are nearly degenerate, the mixing phenomena are strongly affected by the form of the decay matrix $M\Gamma$. In this limit the difference of the Higgs widths determines the modulus as well as the phase of the mixing parameter $X = \frac{1}{2}\tan 2\theta$. Though the partial widths are nearly equal for decays of the two Higgs bosons to top pairs, only the H channel may be open for decays to light Higgs boson pairs. Since the difference of the widths enters through the denominator in X, the modulus $|X|$ becomes large for small differences, and small widths in general.

The mixing shifts the Higgs masses and widths in a characteristic pattern [10]. The two complex mass values after and before diagonalization are related by the complex mixing angle θ:

$$\begin{aligned} & \left[M_{H_3}^2 - {\rm i}M_{H_3}\Gamma_{H_3}\right] \mp \left[M_{H_2}^2 - {\rm i}M_{H_2}\Gamma_{H_2}\right] \\ & = \left\{\left[M_A^2 - {\rm i}M_A\Gamma_A\right] \mp \left[M_H^2 - {\rm i}M_H\Gamma_H\right]\right\} \begin{cases} \times\sqrt{1+4X^2}\,, \\ \times \quad 1\,. \end{cases} \end{aligned} \tag{31}$$

As expected from rotational transformations, which leave the trace of matrices invariant, the complex eigenvalues split in exactly opposite directions when the mixing is switched on.[3]

The individual shifts of masses and widths can easily be obtained by separating real and imaginary parts in the relations:

$$\begin{aligned} & \left[M_{H_2}^2 - {\rm i}M_{H_2}\Gamma_{H_2}\right] - \left[M_H^2 - {\rm i}M_H\Gamma_H\right] \\ & = -\left\{\left[M_{H_3}^2 - {\rm i}M_{H_3}\Gamma_{H_3}\right] - \left[M_A^2 - {\rm i}M_A\Gamma_A\right]\right\}, \\ & = -\left\{\left[M_A^2 - {\rm i}M_A\Gamma_A\right] - \left[M_H^2 - {\rm i}M_H\Gamma_H\right]\right\} \\ & \quad \times \frac{1}{2}\left[\sqrt{1+4X^2} - 1\right]. \end{aligned} \tag{32}$$

If the mixing parameter is small and real, the gap between the states increases quadratically with the size of the mixing; if the mixing is large, linearly.

The eigenstates of the complex, non-hermitian matrix $\mathcal{M}^2_{HA}$ of (27) are no longer orthogonal, but instead

$$\begin{aligned} |H_2\rangle &= \cos\theta\,|H\rangle + \sin\theta\,|A\rangle, \\ |H_3\rangle &= -\sin\theta\,|H\rangle + \cos\theta\,|A\rangle, \\ \langle\widetilde{H}_2| &= \cos\theta\,\langle H| + \sin\theta\,\langle A|, \\ \langle\widetilde{H}_3| &= -\sin\theta\,\langle H| + \cos\theta\,\langle A|\,. \end{aligned} \tag{33}$$

Correspondingly, the final state F in heavy Higgs formation from the initial state I is generated with the transition am-

[3] At the very end of the analysis one may order the Higgs states according to ascending masses in CP-noninvariant theories. However, at intermediate steps the notation used here proves more transparent.

plitude[4]

$$\langle F|H|I\rangle = \sum_{i=2,3} \langle F|H_i\rangle \frac{1}{s - M^2_{H_i} + \mathrm{i}M_{H_i}\Gamma_{H_i}} \langle \widetilde{H}_i|I\rangle. \quad (34)$$

3.1 An illustrative example

We illustrate the mixing mechanism in a simple toy model in which $M_A = 0.5\,\mathrm{TeV}$, $\tan\beta = 5$ and all $|\lambda_i| = 0.4$ [i.e. roughly equal to the weak SU(2) gauge coupling squared], while a common phase ϕ of all the complex parameters $\lambda_{5,6,7}$ is varied from 0 through π to 2π.[5] The scalar and pseudoscalar couplings of the top quark are identified with the standard CP-conserving values $s_H \simeq p_A = \cot\beta\, m_t/v$ and $p_H = s_A = 0$ in the decoupling limit. The mass of the light Higgs boson moves in this toy model from $M_h = 215\,\mathrm{GeV}$ to 161 GeV to 74 GeV as the phase ϕ is varied from 0 through $\pi/2$ to π and, for $\phi = 0$, the masses and widths of the heavy states are $M_{H_2} = M_H = 520\,\mathrm{GeV}$, $M_{H_3} = M_A = 500\,\mathrm{GeV}$, $\Gamma_H = 2.58\,\mathrm{GeV}$ and $\Gamma_A = 1.49\,\mathrm{GeV}$.

For these parameters, the Argand diagram of the mixing parameter X is presented in Fig. 1a in which the common CP-violating phase ϕ evolves from 0 to π [for $\phi > \pi$ the reflection symmetry $\Re\mathrm{e}/\Im\mathrm{m}X \to +\Re\mathrm{e}/-\Im\mathrm{m}X$ at $\phi = \pi$ may be used]; Fig. 1b zooms in on the area of small angles. Alternatively, the real and imaginary parts of X are shown explicitly in Fig. 1c as functions of the common CP-violating phase ϕ.

The difference of the squared masses $M^2_H - M^2_A$ and the real part of the mass mixing parameter Δ^2_{HA} are approximately given by

$$M^2_H - M^2_A = (\lambda - \lambda_A)v^2 \approx \lambda v^2 \cos\phi,$$
$$\Re\mathrm{e}(\Delta^2_{HA}) = \lambda_p v^2 \approx -\frac{1}{2}\lambda\, v^2 \sin\phi, \quad (35)$$

and the imaginary parts by

$$32\pi\,[M_H\Gamma_H - M_A\Gamma_A] \approx \Delta_t + 9\lambda^2 v^2 \cos 2\phi, \quad (36)$$
$$32\pi\,\Im\mathrm{m}\left(\Delta^2_{HA}\right) = 32\pi(M\Gamma)_{HA} \approx -\frac{9}{2}\lambda^2 v^2 \sin 2\phi,$$

for the parameters specified above. Since the complex couplings are parameterized by a phase, $\cos\phi$ enters in the real part of the couplings and thus affects the diagonal elements of the mass matrix. The difference of the imaginary parts of the diagonal elements is determined by the widths of the H/A decays to top quark pairs, $\Delta_t = -12M^2_{H/A}(m_t/v)^2(1-\beta_t^2)\beta_t$, modulated by sinusoidal variations from decays to hh. The modulus of the real part of X rises more rapidly than the imaginary part; $|X|$ reaches unity for a phase $\sim \pi/3$, and the maximum value of about 10 a little below $\phi = \pi/2$ where H and A masses become equal. The Argand diagram is described by a circle to a high degree of accuracy; the center is located on the positive imaginary axis, and the radius of the circle is given by $\sim \lambda v^2/4|M_H\Gamma_H - M_A\Gamma_A| \sim 5$ in the present scenario. Note that the resonant behavior is very sharp as shown in Fig. 1c what is also apparent from the swift move along the circle in the Argand diagram. The ϕ dependence of X follows the typical absorptive/dispersive pattern of analytical resonance amplitudes.

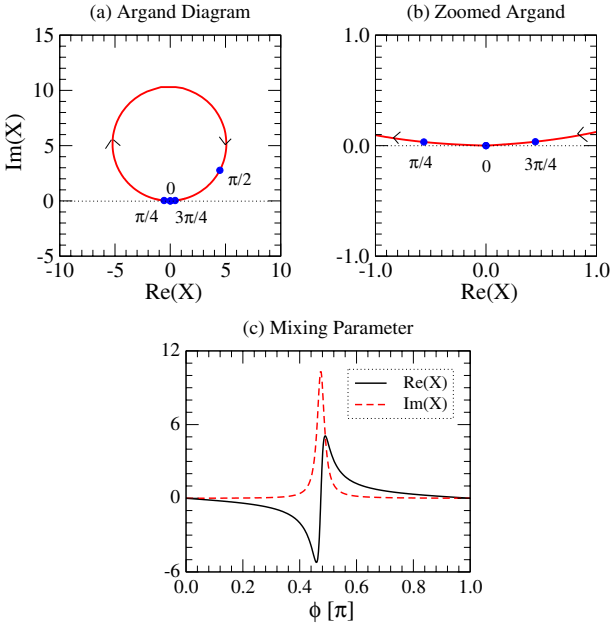

Fig. 1. a,b The Argand diagram and **c** the ϕ dependence of the mixing parameter X in a toy model with the common CP-violating phase ϕ evolving from 0 to π for $\tan\beta = 5$, $M_A = 0.5\,\mathrm{TeV}$ and with all $|\lambda_i| = 0.4$ [$\approx g^2$]; the upper right-hand side zooms in on small angles. Note that $\Re\mathrm{e}/\Im\mathrm{m}X(2\pi - \phi) = +\Re\mathrm{e}/-\Im\mathrm{m}X(\phi)$

The shifts of masses and widths emerging from H and A are displayed in Figs. 2a,b. The differences of masses and widths of H and A without the CP-violating mixing Δ^2_{HA} are shown by the dashed lines. As expected from (35), the overall mass shift decreases monotonically with varying ϕ from 0 to π while the width shift shows an approximate sinusoidal behavior. If $\phi \approx \pi/2$ the H–A mass difference becomes so small that the mixing parameter X can become very large $\sim \mathrm{i}\,\lambda v^2/2\,(M_H\Gamma_H - M_A\Gamma_A) \sim 10\,\mathrm{i}$ in the numerical example. Both CP-conserving quantities are symmetric about $\phi = \pi$. The impact of H/A mixing on the character of ΔM, in particular, is quite significant.

4 A specific SUSY example

To illustrate these general quantum mechanical results in a potentially more realistic example, we shall apply the for-

[4] Small off-resonance transitions of heavy Higgs bosons H and A to the light Higgs boson h (and to the neutral would-be Goldstone G^0) can be neglected in the decoupling limit to a good approximation.

[5] With one common phase ϕ, the complex mixing parameter X obeys the relation $X(2\pi - \phi) = X^*(\phi)$, i.e. $\Re\mathrm{e}/\Im\mathrm{m}X \to +\Re\mathrm{e}/-\Im\mathrm{m}X$. As a result, all CP-even quantities are symmetric and all CP-odd quantities anti-symmetric about π, i.e. when switching from ϕ to $2\pi - \phi$. Therefore we can restrict the discussion to the range $0 \le \phi \le \pi$.

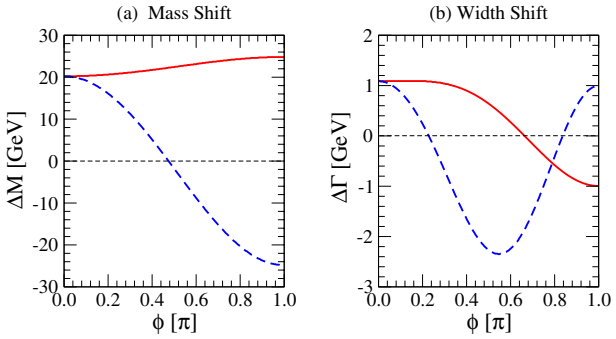

Fig. 2. a,b The dependence of the mass and width shifts, $\Delta M = M_{H_2} - M_{H_3}$ and $\Delta\Gamma = \Gamma_{H_2} - \Gamma_{H_3}$, on the phase ϕ. The dashed lines display these differences without mixing for the H, A states. Both quantities are symmetric about $\phi = \pi$

malism to a specific scenario within the minimal supersymmetric standard model but extended by CP-violating elements [MSSM-CP]. We assume the source of CP-violation to be localized in the complex trilinear coupling A_t of the soft supersymmetry breaking part of the potential involving the top squark.[6] All other interactions are assumed to be CP-conserving.

Through stop-loop corrections CP-violation is transmitted in this scenario to the effective Higgs potential. Expressed in the general form (1), the effective λ parameters have been calculated in [3] to two-loop accuracy; to illustrate the crucial points we recollect the compact one-loop results of the $t/\tilde{t}$ contributions:

$$\lambda_1 = \frac{g^2+g'^2}{4} - \frac{h_t^4}{32\pi^2}\frac{|\mu|^4}{M_S^4},$$

$$\lambda_2 = \frac{g^2+g'^2}{4} + \frac{3h_t^4}{8\pi^2}\left[\log\frac{M_S^2}{m_t^2} + \frac{1}{2}X_t\right],$$

$$\lambda_3 = \frac{g^2-g'^2}{4} + \frac{h_t^4}{32\pi^2}\left(\frac{3|\mu|^2}{M_S^2} - \frac{|\mu|^2|A_t|^2}{M_S^4}\right),$$

$$\lambda_4 = -\frac{g^2}{2} + \frac{h_t^4}{32\pi^2}\left(\frac{3|\mu|^2}{M_S^2} - \frac{|\mu|^2|A_t|^2}{M_S^4}\right),$$

$$\lambda_5 = -\frac{h_t^4}{32\pi^2}\frac{\mu^2 A_t^2}{M_S^4},$$

$$\lambda_6 = \frac{h_t^4}{32\pi^2}\frac{|\mu|^2\mu A_t}{M_S^4},$$

$$\lambda_7 = -\frac{h_t^4}{32\pi^2}\frac{\mu}{M_S}\left(\frac{6A_t}{M_S} - \frac{|A_t|^2 A_t}{M_S^3}\right), \qquad (37)$$

where

$$h_t = \frac{\sqrt{2}\overline{m}_t(m_t)}{v\sin\beta} \text{ and } X_t = \frac{2|A_t|^2}{M_S^2}\left(1 - \frac{|A_t|^2}{12M_S^2}\right). \qquad (38)$$

[6] This assignment is compatible with the bounds on CP-violating SUSY phases derived from experiments on electric dipole moments [12].

Here, m_t is the top quark pole mass related to the running $\overline{MS}$ mass $\overline{m}_t(m_t)$ through $\overline{m}_t(m_t) = m_t/\left[1 + \frac{4}{3\pi}\alpha_s(m_t)\right]$, and M_S is the SUSY scale.

These λ parameters determine the effective potential from which the one-loop improved Born Higgs mass matrix is derived. By including dispersive contributions from Higgs self-energies, the matrix elements are shifted to the pole-mass parameters. In the decoupling limit for heavy Higgs masses and very heavy masses of the supersymmetric particles, top quark loops build up the self-energy contributions. The shifts are individually small for scalar and pseudoscalar Higgs masses in this limit. Moreover, since the mixing parameter X is affected only by the mass difference, the shifts cancel in X asymptotically in the chirally symmetric decoupling limit. For the set of parameters chosen subsequently for illustration, these effects are very small, $O(100\,\text{MeV})$, and we will ignore them in the numerical analysis.

To demonstrate the complex H/A mixing in this MSSM-CP model numerically, we adopt a typical set of parameters from [4,13],

$$M_S = 0.5\,\text{TeV}, \quad |A_t| = 1.0\,\text{TeV}, \quad \mu = 1.0\,\text{TeV};$$
$$\tan\beta = 5, \qquad (39)$$

while varying the phase ϕ_A of the trilinear parameter A_t.

In the CP-conserving case with $\phi_A = 0$ we find the following values of the light and heavy Higgs masses and decay widths:

$$M_h = 129.6\,\text{GeV}, \; M_H = 500.3\,\text{GeV}, \; M_A = 500.0\,\text{GeV},$$
$$\Gamma_H = 1.2\,\text{GeV}, \quad \Gamma_A = 1.5\,\text{GeV}, \qquad (40)$$

and the stop masses:

$$m_{\tilde{t}_1} = 372\,\text{GeV}, \quad m_{\tilde{t}_2} = 647\,\text{GeV}. \qquad (41)$$

While the light Higgs boson mass is not altered if CP-violation through the phase ϕ_A is turned on, the Argand diagram and the variation of the CP-violating parameter X are presented in Figs. 3a,b,c. [Symmetries in moving from ϕ_A to $2\pi - \phi_A$ are identical to the toy model.] The mass and width shifts of the heavy neutral Higgs bosons are displayed in Figs. 4a,b, respectively. Similar to the toy model in the previous section, the two-state system in the MSSM-CP shows a very sharp resonant CP-violating mixing, purely imaginary a little above $\phi_A = 3\pi/4$. The mass shift is enhanced by more than an order of magnitude if the CP-violating phase rises to non-zero values, reaching a maximal value of $\sim 5.3\,\text{GeV}$; the width shift moves up [non-uniformly] from -0.3 and $+0.4\,\text{GeV}$. As a result, the two mass eigenstates become clearly distinguishable, incorporating significant admixtures of CP-even and CP-odd components mutually in the wave-functions.

5 Experimental signatures of CP-mixing

(i) A first interesting example for studying CP-violating mixing effects is provided by $\gamma\gamma$–*Higgs formation in polarized beams* [14–16]:

$$\gamma\gamma \to H_i \quad [i = 2, 3]\,. \qquad (42)$$

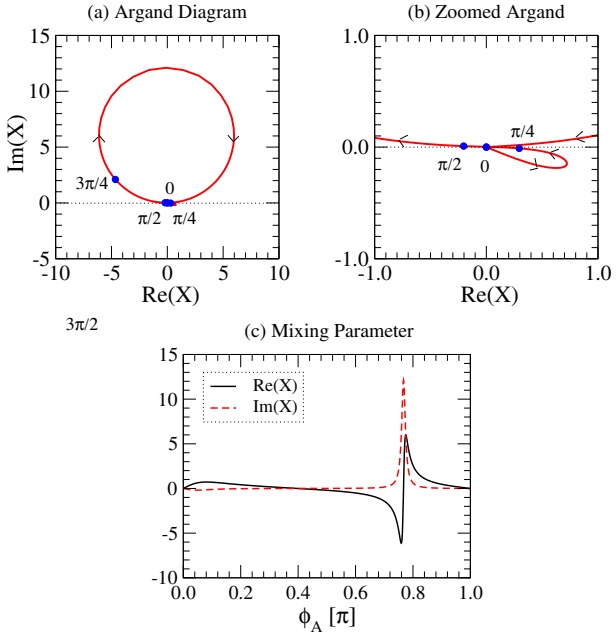

Fig. 3. a,b The Argand diagram and **c** the ϕ_A dependence of the mixing parameter X in a SUSY model with the CP-violating phase ϕ_A evolving from 0 to π for $\tan\beta = 5$, $M_A = 0.5$ TeV and couplings as specified in the text; the Argand diagram zoomed in on small angles is displayed on the upper right-hand frame. $\Re\mathrm{e}/\Im\mathrm{m}X(2\pi - \phi_A) = +\Re\mathrm{e}/-\Im\mathrm{m}X(\phi_A)$ for angles above π

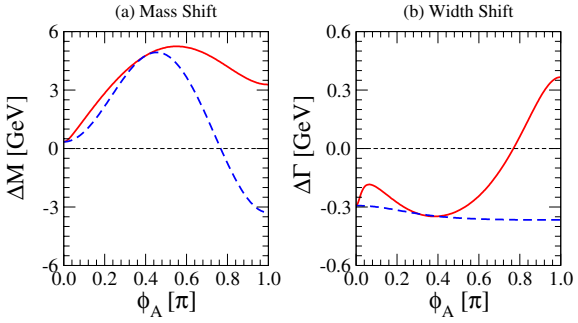

Fig. 4. a,b The dependence of the shifts of masses and widths on the CP-violating angle ϕ_A in the SUSY model with the same parameter set as in Fig. 3; the differences without mixing are shown by the dashed lines

For a specific final state F of the Higgs boson decays, the amplitude of the reaction $\gamma\gamma \to H_i \to F$ is a superposition of H_2 and H_3 exchanges. For helicities $\lambda = \pm 1$ of the two photons, the amplitude reads

$$\mathcal{M}^F_\lambda = \sum_{i=2,3} \langle F|H_i\rangle\, D_i(s)\, \left[S^\gamma_i(s) + \mathrm{i}\lambda P^\gamma_i(s)\right] . \qquad (43)$$

The loop-induced $\gamma\gamma H_i$ amplitudes are described by the scalar and pseudoscalar form factors, $S^\gamma_i(s)$ and $P^\gamma_i(s)$ where $\sqrt{s}$ is the $\gamma\gamma$ energy and the Higgs H_i propagator reads $D_i(s) = 1/\left(s - M^2_{H_i} + \mathrm{i}M_{H_i}\Gamma_{H_i}\right)$ in the Breit–Wigner form. The scalar and pseudoscalar form factors receive the *dominant* contributions from the top (s)quark loops in the decoupling regime for moderate values of $\tan\beta$ [while bottom loops are suppressed by the Yukawa coupling and the small electric b charge]. These form factors are related to the well-known conventional $\gamma\gamma H/A$ form factors, $S^\gamma_{H,A}$ and $P^\gamma_{H,A}$, by

$$\begin{aligned} S^\gamma_2 &= \cos\theta\, S^\gamma_H + \sin\theta\, S^\gamma_A, \quad S^\gamma_3 = -\sin\theta\, S^\gamma_H + \cos\theta\, S^\gamma_A, \\ P^\gamma_2 &= \cos\theta\, P^\gamma_H + \sin\theta\, P^\gamma_A, \quad P^\gamma_3 = -\sin\theta\, P^\gamma_H + \cos\theta\, P^\gamma_A . \end{aligned} \qquad (44)$$

For the explicit form of the loop functions $S^\gamma_{H,A}$ and $P^\gamma_{H,A}$ see, for example, [13]. To reduce technicalities, the Higgs–tt couplings are assumed to be CP-conserving, implying no top-loop contributions to P^γ_H and S^γ_A. This simplifying assumption is approximately realized in scenarios in which the gluino mass is sufficiently heavy compared with the stop masses [5]. The $\tilde{t}_1$ loop, with non-vanishing $A\tilde{t}_1\tilde{t}_1$ coupling, may generate a CP-violating form factor S^γ_A. However, in the region of strong mixing on which the present analysis is focused, the CP-violating vertex corrections have only a small effect on the experimental asymmetries compared with the large impact of CP-violating Higgs–boson mixing. [The assumption can easily be removed if general MSSM-CP scenarios are analyzed beyond the present generic level.] The relevant production rates for heavy SUSY Higgs bosons have been calculated in [17].

For linearly polarized photons, the CP-even component of the H_i wave-functions is projected out if the polarization vectors are parallel, and the CP-odd component if they are perpendicular. This effect can be observed in the CP-even asymmetry

$$\mathcal{A}_{\mathrm{lin}} = \frac{\sigma_\parallel - \sigma_\perp}{\sigma_\parallel + \sigma_\perp} \qquad (45)$$

of the total $\gamma\gamma$ fusion cross sections for linearly polarized photons. Though not CP-violating *sui generis*, the asymmetry $\mathcal{A}_{\mathrm{lin}}$ provides us with a powerful tool nevertheless to probe CP-violating admixtures to the Higgs states since $|\mathcal{A}_{\mathrm{lin}}| < 1$ requires both S^γ_i and P^γ_i non-zero couplings. Moreover, CP-violation due to H/A mixing can directly be probed via the CP-odd asymmetry[7] constructed with circular photon polarization as

$$\mathcal{A}_{\mathrm{hel}} = \frac{\sigma_{++} - \sigma_{--}}{\sigma_{++} + \sigma_{--}} . \qquad (46)$$

The upper panels of Fig. 5 show the ϕ_A dependence of the asymmetries $\mathcal{A}_{\mathrm{lin}}$ and $\mathcal{A}_{\mathrm{hel}}$ at the poles of H_2 and of H_3, respectively, for the same parameter set as in Fig. 3 and with the common SUSY scale $M_{\tilde{Q}_3} = M_{\tilde{t}_{\mathrm{R}}} = M_S = 0.5$ TeV for the soft SUSY breaking top squark mass parameters.[8] By

[7] This asymmetry is also odd under $CP\tilde{T}$ where the naive time reversal transformation $\tilde{T}$ [18] reverses the direction of all 3-momenta and spins, but does not exchange initial and final state. Quantities that are odd under $CP\tilde{T}$ can be non-zero only for complex transition amplitudes with absorptive phases which can be generated, for example, by loops, and Breit–Wigner propagators.

[8] On quite general grounds, the CP-conserving observables are symmetric under the reflection about $\phi_A = \pi$, while the CP-violating observables are anti-symmetric.

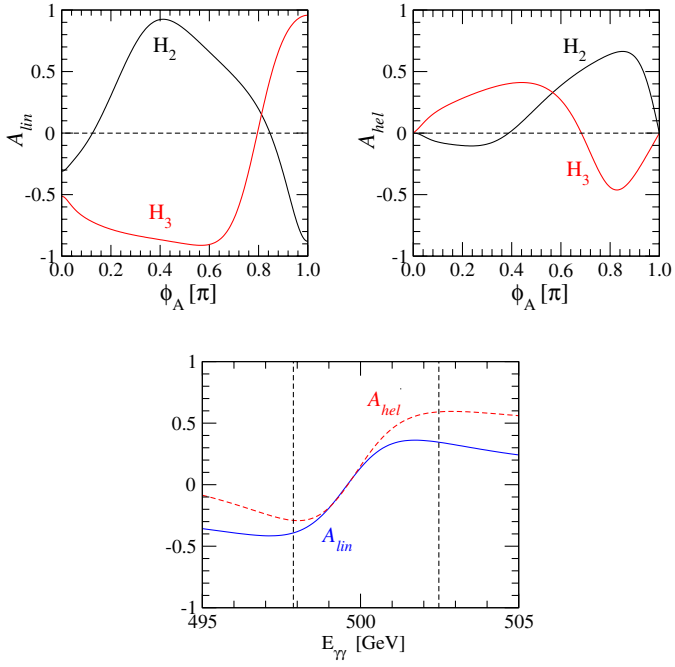

Fig. 5. The ϕ_A dependence of the CP-even and CP-odd correlators, $\mathcal{A}_{\rm lin}$ (upper-left panel) and $\mathcal{A}_{\rm hel}$ (upper-right panel), at the poles of H_2 and H_3, respectively, and the $\gamma\gamma$ energy dependence (lower panel) of the correlators, $\mathcal{A}_{\rm lin,hel}$ for $\phi_A = 3\pi/4$ in the production process $\gamma\gamma \to H_i$ in the limit in which H/A mixing is the dominant CP-violating effect. The same parameter set as in Fig. 3 is employed. Numerically, $M_{H_2} = 502.5\,\text{GeV}$, $M_{H_3} = 497.9\,\text{GeV}$, $\Gamma_{H_2} = 1.28\,\text{GeV}$ and $\Gamma_{H_3} = 1.31\,\text{GeV}$. The vertical lines on the lower panel represent the two mass eigenvalues, M_{H_3} and M_{H_2}

varying the $\gamma\gamma$ energy from below M_{H_3} to above M_{H_2}, the asymmetries, $\mathcal{A}_{\rm lin}$ (blue solid line) and $\mathcal{A}_{\rm hel}$ (red dashed line), vary from -0.39 to 0.34 and from -0.29 to 0.59, respectively, as demonstrated on the lower panel of Fig. 5 with $\phi_A = 3\pi/4$, a phase value close to resonant CP-mixing.

If the widths are neglected, the asymmetries $\mathcal{A}_{\rm lin}$ and $\mathcal{A}_{\rm hel}$ on top of the H_i $[i = 2, 3]$ poles can approximately be written in terms of the form factors:

$$\mathcal{A}_{\rm lin}[H_i] \approx \frac{|S_i^\gamma|^2 - |P_i^\gamma|^2}{|S_i^\gamma|^2 + |P_i^\gamma|^2}, \tag{47}$$

$$\mathcal{A}_{\rm hel}[H_i] \approx \frac{2\,\Im\text{m}\left(S_i^\gamma P_i^{\gamma *}\right)}{|S_i^\gamma|^2 + |P_i^\gamma|^2}. \tag{48}$$

These approximate formulae reproduce the numerical values very accurately. If one further neglects not only small corrections due to such overlap phenomena but also corrections due to non-asymptotic Higgs-mass values, the asymmetries on top of the H_2 and H_3 poles can simply be expressed by the complex mixing angle θ:

$$\mathcal{A}_{\rm lin}[H_2] \simeq -\mathcal{A}_{\rm lin}[H_3] \simeq \frac{|\cos\theta|^2 - |\sin\theta|^2}{|\cos\theta|^2 + |\sin\theta|^2}, \tag{49}$$

$$\mathcal{A}_{\rm hel}[H_2] \simeq +\mathcal{A}_{\rm hel}[H_3] \simeq \frac{2\,\Im\text{m}\,(\cos\theta \sin\theta^*)}{|\cos\theta|^2 + |\sin\theta|^2}. \tag{50}$$

The asymmetries $\mathcal{A}_{\rm lin}$ are opposite in sign for the two Higgs bosons H_2 and H_3, while the asymmetries $\mathcal{A}_{\rm hel}$ have the same sign. However, we note that the corrections due to non-asymptotic Higgs masses are still quite significant for the mass ratio $M_{H_2,H_3}/2m_t \sim 1.3$ in our reference point, particularly for $\mathcal{A}_{\rm hel}$ which is sensitive to the interference between the $\gamma\gamma H$ and $\gamma\gamma A$ form factors[9].

Detailed experimental simulations would be needed to estimate the accuracy with which the asymmetries can be measured. However, the large magnitude and the rapid, significant variation of the CP-even and CP-odd asymmetries, $\mathcal{A}_{\rm lin}$ and $\mathcal{A}_{\rm hel}$, through the resonance region with respect to both the phase ϕ_A and the $\gamma\gamma$ energy would be a very interesting effect to observe in any case.

(ii) A second observable of interest for studying CP-violating mixing effects experimentally is the *polarization of the top quarks in H_i decays* produced by $\gamma\gamma$ fusion [14,19] or elsewhere in various production processes at an e^+e^- linear collider and LHC:

$$H_i \to t\bar{t} \quad [i = 2, 3]. \tag{51}$$

Even if the H/Att couplings are [approximately] CP-conserving, the complex rotation matrix C may mix the CP-even H and CP-odd A states leading to the CP-violating helicity amplitude of the decay process $H_i \to t\bar{t}$:

$$\langle t_\sigma \bar{t}_\sigma | H_i \rangle = \sum_{a=H,A} C_{ia}(\sigma\beta_t s_a - \text{i}p_a), \tag{52}$$

where the t and $\bar{t}$ helicities $\sigma/2 = \pm 1/2$ must be equal and s_a, p_a are the Htt and Att couplings defined in (19). The two correlations between the transverse t and $\bar{t}$ polarization vectors $s_\perp, \bar{s}_\perp$ in the production-decay process $\gamma\gamma \to H_i \to t\bar{t}$,

$$\mathcal{C}_\parallel = \langle s_\perp \cdot \bar{s}_\perp \rangle \qquad \text{and} \qquad \mathcal{C}_\perp = \langle \hat{p}_t \cdot (s_\perp \times \bar{s}_\perp) \rangle \tag{53}$$

lead to a non-trivial CP-even/$CP\tilde{T}$-even azimuthal correlation and a different CP-odd/$CP\tilde{T}$-even azimuthal correlation between the two decay planes $t \to bW^+$ and $\bar{t} \to \bar{b}W^-$:

$$\frac{1}{\Gamma}\frac{\text{d}\Gamma}{\text{d}\phi^*} = \frac{1}{2\pi}\left[1 - \frac{\pi^2}{16}\left(\frac{1 - 2m_W^2/m_t^2}{1 + 2m_W^2/m_t^2}\right)^2 \times \left(\mathcal{C}_\parallel \cos\phi^* + \mathcal{C}_\perp \sin\phi^*\right)\right], \tag{54}$$

where ϕ^* denotes the azimuthal angle between two decay planes [14]. In terms of the helicity amplitudes $\langle\sigma, \lambda\rangle$ for the process $\gamma\gamma \to H_i \to t\bar{t}$, where $\lambda = \pm 1$ denotes the helicities of both photons and $\sigma = \pm 1$ twice the helicities of both top quarks, the asymmetries are given as

$$\mathcal{C}_\parallel = -\frac{2\,\Re\text{e}\sum\langle +, \lambda\rangle\langle -, \lambda\rangle^*}{\sum\left(|\langle +, \lambda\rangle|^2 + |\langle -, \lambda\rangle|^2\right)}, \tag{55}$$

$$\mathcal{C}_\perp = +\frac{2\,\Im\text{m}\sum\langle +, \lambda\rangle\langle -, \lambda\rangle^*}{\sum\left(|\langle +, \lambda\rangle|^2 + |\langle -, \lambda\rangle|^2\right)}, \tag{56}$$

with the sums running over the two photon helicities.

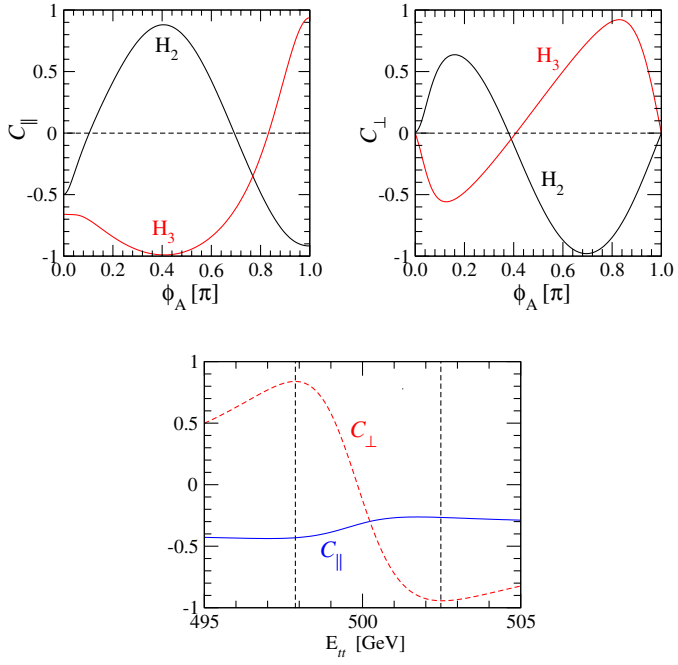

Fig. 6. The ϕ_A dependence of the CP-even and CP-odd correlators, $\mathcal{C}_\parallel$ (upper-left panel) and $\mathcal{C}_\perp$ (upper-right panel), at the pole of H_2 and H_3 and the invariant $t\bar{t}$ energy dependence (lower panel) of the correlators $\mathcal{C}_{\parallel,\perp}$ for $\phi_A = 3\pi/4$ in the production–decay chain $\gamma\gamma \to H_i \to t\bar{t}$. [Same SUSY parameter set as in Fig. 5]

The upper panels of Fig. 6 show the ϕ_A dependence of the CP-even and CP-odd asymmetries, $\mathcal{C}_\parallel$ and $\mathcal{C}_\perp$, at the poles of H_2 and of H_3, respectively, for the same parameter set as in Fig. 5. If the invariant $t\bar{t}$ energy is varied throughout the resonance region, the correlators $\mathcal{C}_\parallel$ (blue solid line) and $\mathcal{C}_\perp$ (red dashed line) vary characteristically from -0.43 to -0.27 [non-uniformly] and from 0.84 to -0.94, respectively, as shown on the lower panel of Fig. 6.

Similarly to the previous case, if the widths are neglected, the $\mathcal{C}_\parallel$ and $\mathcal{C}_\perp$ asymmetries on top of the H_2 and H_3 poles can approximately be expressed by the complex mixing angle θ as

$$\mathcal{C}_\parallel[H_2] \simeq \frac{|\cos\theta|^2\beta_t^2 - |\sin\theta|^2}{|\cos\theta|^2\beta_t^2 + |\sin\theta|^2},$$

$$\mathcal{C}_\parallel[H_3] \simeq -\frac{|\cos\theta|^2 - |\sin\theta|^2\beta_t^2}{|\cos\theta|^2 + |\sin\theta|^2\beta_t^2}, \qquad (57)$$

$$\mathcal{C}_\perp[H_2] \simeq \frac{2\Re\mathrm{e}(\cos\theta\sin\theta^*)\beta_t}{|\cos\theta|^2\beta_t^2 + |\sin\theta|^2},$$

$$\mathcal{C}_\perp[H_3] \simeq -\frac{2\Re\mathrm{e}(\cos\theta\sin\theta^*)\beta_t}{|\cos\theta|^2 + |\sin\theta|^2\beta_t^2}. \qquad (58)$$

These approximate formulae provide a nice qualitative understanding of the numerical values. In the asymptotic kinematic limit $\beta_t \to 1$ of the top quark velocity, the correlators reduce to the simple expressions:

$$\mathcal{C}_\parallel[H_2] \simeq -\mathcal{C}_\parallel[H_3] \simeq \frac{|\cos\theta|^2 - |\sin\theta|^2}{|\cos\theta|^2 + |\sin\theta|^2}, \qquad (59)$$

$$\mathcal{C}_\perp[H_2] \simeq -\mathcal{C}_\perp[H_3] \simeq \frac{2\,\Re\mathrm{e}(\cos\theta\sin\theta^*)}{|\cos\theta|^2 + |\sin\theta|^2}, \qquad (60)$$

i.e. they are both opposite in sign. However, we note that the square of the top quark velocity $\beta_t^2 \approx 0.5$ near the Higgs resonances so that the corrections due to non-asymptotic Higgs masses are significant, in particular, for the asymmetry $\mathcal{C}_\parallel$ in the present example.

Though not easy to observe, the gross effects, at least, in Fig. 6 should certainly be accessible experimentally.

6 Conclusions

Exciting mixing effects can occur in the Higgs sector of 2-Higgs doublet models, *nota bene* in supersymmetric models, if CP-noninvariant interactions are switched on. In the decoupling regime these effects can become very large, leading to interesting experimental consequences. We have analyzed such scenarios in a general quantum mechanical language that provides us with a clear and transparent understanding of the phenomena in the general two-doublet model. Moreover, the effects are illustrated in the minimal supersymmetric standard model extended by CP-violating interactions [MSSM-CP]. Higgs formation in $\gamma\gamma$ collisions proves particularly interesting for observing such effects. However, exciting experimental effects are also predicted in such scenarios for $t\bar{t}$ final-state analyses in decays of the heavy Higgs bosons at LHC and in the e^+e^- mode of linear colliders.

Acknowledgements. We thank G.A. Blair and M. Drees for valuable remarks. Special thanks go to M. Carena for the careful reading of the manuscript and suggested corrections. The work is supported in part by the European Commission 5th Framework Contract HPRN-CT-2000-00149. SYC was supported in part by a Korea Research Foundation Grant (KRF-2002-070-C00022) and in part by KOSEF through CHEP at Kyungpook National University. JK was supported by the KBN Grant 2 P02B 040 24 (2003–2005) and 115/E-343/SPB/DESY/P-03/DWM517/2003–2005.

References

1. J.F. Gunion, B. Grzadkowski, H.E. Haber, J. Kalinowski, Phys. Rev. Lett. **79**, 982 (1997); B. Grzadkowski, J.F. Gunion, J. Kalinowski, Phys. Rev. D **60**, 075011 (1999)
2. A. Pilaftsis, Phys. Rev. D **58**, 096010 (1998); Phys. Lett. B **435**, 88 (1998)
3. A. Pilaftsis, C.E.M. Wagner, Nucl. Phys. B **553**, 3 (1999)
4. D.A. Demir, Phys. Rev. D **60**, 055006 (1999); S.Y. Choi, M. Drees, J.S. Lee, Phys. Lett. B **481**, 57 (2000) and earlier references
5. M. Carena, J. Ellis, A. Pilaftsis, C.E.M. Wagner, Nucl. Phys. B **586**, 92 (2000); Nucl. Phys. B **625**, 345 (2002)

[9] We have checked that indeed the numerical values approach formula (50) for very large Higgs masses.

6. J.F. Gunion, H.E. Haber, Phys. Rev. D **67**, 075019 (2003)
7. J.F. Gunion, H.E. Haber, J. Kalinowski, in preparation. For another point of view see also I.F. Ginzburg, M. Krawczyk, P. Osland, hep-ph/0211371; M.N. Dubinin, A.V. Semenov, Eur. Phys. J. C **28**, 233 (2003)
8. V.F. Weisskopf, E.P. Wigner, Z. Phys. **63**, 54 (1930); **65**, 1113 (1930)
9. D.J. Miller, R. Nevzorov, P.M. Zerwas, Nucl. Phys. B **681**, 3 (2004); S.Y. Choi, D.J. Miller, P.M. Zerwas, DESY 04-088, and hep-ph/0407209
10. S. Güsken, J.H. Kühn, P.M. Zerwas, Nucl. Phys. B **262**, 393 (1985)
11. A. Pilaftsis, Z. Phys. C **47**, 95 (1990); A. Pilaftsis, M. Nowakowski, Mod. Phys. Lett. A **6**, 1933 (1991); Phys. Lett. B **245**, 185 (1990); A. Pilaftsis, Phys. Rev. Lett. **77**, 4996 (1996); Nucl. Phys. B **504**, 61 (1997); J. Ellis, J.S. Lee, A. Pilaftsis, hep-ph/0404167
12. Y. Kizukuri, N. Oshimo, Phys. Lett. B **249**, 449 (1990); I. Ibrahim, P. Nath, Phys. Rev. D **58**, 111301 (1998); **60**, 099902(E) (1998); **61**, 093004 (2000); M. Brhlik, G.J. Good, G.L. Kane, Phys. Rev. D **59**, 115004 (1999); R. Arnowitt, B. Dutta, Y. Santos, Phys. Rev. D **64**, 113010 (2000); V. Barger, T. Falk, T. Han, J. Jiang, T. Li, T. Plehn, Phys. Rev. D **64**, 056007 (2001); S.Y. Choi, M. Drees, B. Gaissmaier, hep-ph/0403054
13. J.S. Lee, A. Pilaftsis, M. Carena, S.Y. Choi, M. Drees, J. Ellis, C.E.M. Wagner, Comp. Phys. Comm. **156**, 283 (2004)
14. M. Krämer, J.H. Kühn, M.L. Stong, P.M. Zerwas, Z. Phys. C **64**, 21 (1994) and references therein; J.I. Illana, hep-ph/9912467
15. B. Grzadkowski, J.F. Gunion, Phys. Lett. B **294**, 361 (1992); S.Y. Choi, J.S. Lee, Phys. Rev. D **62**, 036005 (2000); E. Asakawa, J. Kamoshita, A. Sugamoto, I. Watanabe, Eur. Phys. J. C **14**, 335 (2000); E. Asakawa, S.Y. Choi, K. Hagiwara, J.S. Lee, Phys. Rev. D **62**, 115005 (2000); E. Asakawa, K. Hagiwara, Eur. Phys. J. C **31**, 351 (2003); R.M. Godbole, S.D. Rindani, R.K. Singh, Phys. Rev. D **67**, 095009 (2003); P. Niezurawski, A.F. Zarnecki, M. Krawczyk, hep-ph/0307180 and hep-ph/0403138
16. B. Badelek et al. [ECFA/DESY Photon Collider Working Group], TESLA-TDR, DESY 01-011FA [hep-ex/0108012]; E. Boos et al., Nucl. Instrum. Methods A **472**, 100 (2001)
17. M.M. Mühlleitner, M. Krämer, M. Spira, P.M. Zerwas, Phys. Lett. B **508**, 311 (2001)
18. A. De Rújula, J.M. Kaplan, E. de Rafael, Nucl. Phys. B **35**, 365 (1971); see also K. Hagiwara, R.D. Peccei, D. Zeppenfeld, K. Hikasa, Nucl. Phys. B **282**, 253 (1987)
19. B. Grzadkowski, J.F. Gunion, Phys. Lett. B **350**, 218 (1995); J.F. Gunion, B. Grzadkowski, X.G. He, Phys. Rev. Lett. **77**, 5172 (1996)